RSC Advances

PAPER

View Article Online
View Journal | View Issue

Check for updates

Cite this: *RSC Adv.*, 2020, **10**, 533

Gold dipyrrin-bisphenolates: a combined experimental and DFT study of metal–ligand interactions†

Kolle E. Thomas,[a] Nicolas Desbois,[b] Jeanet Conradie,[ac] Simon J. Teat,[d] Claude P. Gros *[b] and Abhik Ghosh *[a]

Received 7th November 2019
Accepted 18th December 2019

DOI: 10.1039/c9ra09228e

rsc.li/rsc-advances

Given that noninnocent and metalloradical-type electronic structures are ubiquitous among dipyrrin-bisphenolate (DPP) complexes, we synthesized the gold(III) derivatives as potentially innocent paradigms against which the properties of other metallo-DPP derivatives can be evaluated. Electronic absorption spectra, electrochemical studies, a single-crystal X-ray structure, and DFT calculations all suggest that the ground states of the new complexes indeed correspond to an innocent Au^{III}–DPP^{3-}, paralleling a similar description noted for Au corroles. Interestingly, while DFT calculations indicate purely ligand-centered oxidations, reduction of AuDPP is predicted to occur across both the metal and the ligand.

1. Introduction

The dipyrrin-bisphenols (H_3DPP) are an emerging class of ligands that share a number of similarities with corroles (Fig. 1).[1] Thus, they are triprotic, afford a square-planar environment for coordinated metals, and even exhibit redox-active behavior remarkably similar to that of corroles.[2,3] Thus, like their corrole analogues,[4–6] a number of M[DPP] derivatives (M = Co,[7,8] Ni,[7] Cu[9]) are best regarded as M^{II}–$L^{\bullet 2-}$, as opposed to M^{III}–L^{3-}. These similarities promise applications of M[DPP] derivatives in catalytic transformations, in which metallocorroles have already proved useful.[10,11] To better understand the role of metalloradical or noninnocent states in DPP chemistry, we have for some time sought innocent M[DPP] complexes, whose properties can serve as standards against which other DPP derivatives can be evaluated. Given that gold(III) corroles have emerged as archetypes of innocent metallocorroles,[12–15] we synthesized a series of gold(III) dipyrrin-bisphenolate derivatives, which, as described below, also appear to exhibit innocent Au^{III}–DPP^{3-} ground states.

2. Results and discussion

2.1 Physical measurements

Three Au(III) *meso-para*-X-phenyl dipyrrin-bisphenolate complexes Au[XDPP] with X = CF_3, H, and Me were obtained as blue solids in 50–77% yields *via* the interaction of the corresponding free ligands and a threefold molar excess of Au(III) acetate in pyridine.[12] A single-crystal X-ray structure (Table 1 and Fig. 2) could be obtained for one of the complexes (X = CF_3). The X-ray structure reveals Au–N/O distances of around 1.97 Å, which are approximately 0.02–0.03 Å longer than Au–N distances typically observed for Au(III) corroles.[12–15] An examination of the skeletal bond distances of Au[CF_3DPP] led to the interesting observation that the C–C bonds in the phenolate moieties span a narrower range (~0.04 Å) relative to M(DPP) derivatives (~0.08 Å) that are unambiguously describable as metalloradicals, as for M = Cu (CCSD: FICCEC, FICCUS)[16] and Pt (LACCUQ, LACDAX).[17] Similarly narrow C–C bond distance ranges are also observed for nonradicaloid Ge (VIVNAR, PONGOQ, SIRFOQ),[18] Mn (UTOVEF[19] and EXOBAV[20]), Al (NABFII),[21–23] Ga (WOMPAS),[24] and In (WOMPIA)[24] DPP complexes.

The three Au complexes exhibit similar optical spectra, with the strongest absorption occurring in the red at 639 ± 5 nm (Fig. 3). The molar absorptivities turned out to be around 3.0×10^4 M^{-1} cm^{-1}, over three times the value observed for Cu[CF_3DPP], consistent with an innocent electronic-structural description for the Au complexes and a radical description for the Cu complex (Fig. 4).[25,26]

Cyclic voltammetric measurements, indicating relatively high oxidation potentials of around +0.95 V against the saturated calomel electrode (SCE),[27] relatively low reduction potentials of around −0.90 V, and substantial electrochemical HOMO–LUMO gaps of around 1.85 V, are also suggestive of an

[a]*Department of Chemistry, UiT – The Arctic University of Norway, Tromsø N-9037, Norway*

[b]*Institut de Chimie Moléculaire de l'Université de Bourgogne (ICMUB), UMR CNRS 6302, Université Bourgogne-Franche Comté, 9 Avenue Alain Savary, BP 47870, 21078 Dijon Cedex, France*

[c]*Department of Chemistry, University of the Free State, Bloemfontein 9300, Republic of South Africa*

[d]*Advanced Light Source, Lawrence Berkeley National Laboratory, Berkeley, California 94720-8229, USA*

† Electronic supplementary information (ESI) available. CCDC 1964008. For ESI and crystallographic data in CIF or other electronic format see DOI: 10.1039/c9ra09228e

Open Access Article. Published on 02 January 2020. Downloaded on 2/22/2026 5:21:19 AM.
This article is licensed under a Creative Commons Attribution-NonCommercial 3.0 Unported Licence.

Open Access Article. Published on 02 January 2020. Downloaded on 2/22/2026 5:21:19 AM.
This article is licensed under a Creative Commons Attribution-NonCommercial 3.0 Unported Licence.

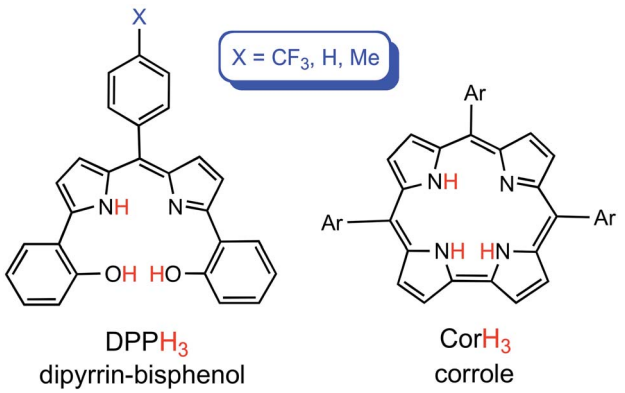

Fig. 1 Free-base dipyrrin-bisphenol and *meso*-triarylcorrole ligands.

innocent description for the Au[XDPP] complexes (Fig. 5). In contrast, Cu[CF_3DPP] (Fig. 6) was found to exhibit an electrochemical HOMO–LUMO gap of just under 1.0 V (qualitatively consistent with similar observations elsewhere[9]). These electrochemical trends closely mirror those observed for analogous coinage metal corroles.[6a,d,g,h,12,15b]

2.2 DFT calculations

To obtain a unified interpretation of the above findings, we carried out scalar-relativistic DFT (OLYP[28,29]/STO-TZ2P) calculations on the *para*-unsubstituted complexes M(DPP) for M = Cu and Au. For Cu, the ground state turned out to be a triplet, consistent with a Cu^{II}–$L^{\cdot 2-}$ description.[9] For Au, the ground state was unambiguously a singlet, with the triplet approximately 1.1 eV higher in energy. Fig. 7, which juxtaposes the optimized skeletal bond distances in the Cu- and Au-DPP complexes, confirms that the phenolate C–C bonds in the Au complex span a significantly smaller range than those in Cu[DPP].

An examination of the Kohn–Sham frontier orbitals of Au[DPP] and their eigenvalues showed that while the ligand-based HOMO is energetically well-separated from the other MOs, the two LUMOs – a DPP-based π-symmetry MO and an Au $5d_{x^2-y^2}$-based σ-symmetry MO – are near-degenerate under C_{2v} symmetry (Fig. 8). Relaxing the point group symmetry to C_2 allows the two LUMOs to mix, as is clear from both the HOMO and spin density profiles of the Au[DPP]$^-$ anion. Thus, while confirming pure ligand-centered oxidation,[30] the calculations provide a more nuanced picture of the reduction process, which occurs over both the Au and the DPP ligand (Fig. 9). In this respect, the Au–DPP complexes differ from simple Au corroles, which exhibit purely ligand-centered reduction.[31] Presumably, the open-chain DPP ligands afford a more flexible coordination cavity for a larger, reduced Au center relative to the much more sterically constrained corroles.

Table 1 Crystal data and structure refinement for Au[CF_3DPP]

Sample	Name
Chemical formula	$C_{28}H_{16}AuF_3N_2O_2$
Formula mass	666.39
Crystal system	Monoclinic
Crystal size (mm^3)	0.090 × 0.040 × 0.020
Space group	$P2_1/c$
λ (Å)	0.7288
a (Å)	6.8844(4)
b (Å)	16.4488(8)
c (Å)	19.8240(10)
α (°)	90
β (°)	98.802(2)
γ (°)	90
Z	4
V ($Å^3$)	2218.4(2)
Temperature (K)	100(2)
Density (calculated)	1.995 Mg m^{-3}
Measured reflections	89 167
Unique reflections	8107
Parameters	0
Restraints	325
R_{int}	0.0502
θ range (°)	2.482 to 33.562
*R*1, w*R*2 all data	0.0462, 0.1131
S (*GooF*) all data	1.332
Max/min res. dens. (e $Å^{-3}$)	3.137/−2.242

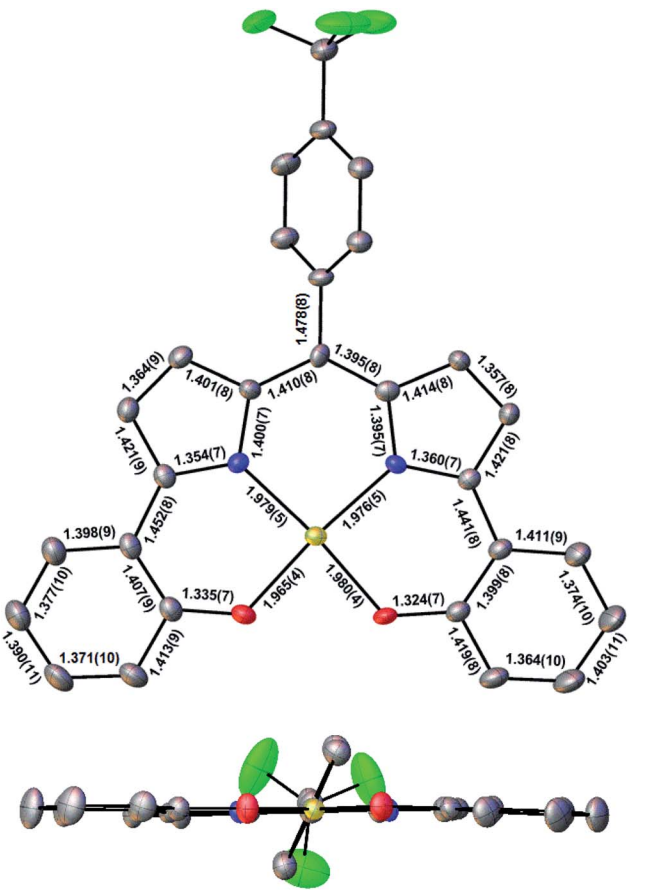

Fig. 2 Molecular structure of Au[CF_3DPP]: top view (above) with selected distances (Å) and side view (below).

This journal is © The Royal Society of Chemistry 2020

Open Access Article. Published on 02 January 2020. Downloaded on 2/22/2026 5:21:19 AM.
This article is licensed under a Creative Commons Attribution-NonCommercial 3.0 Unported Licence.

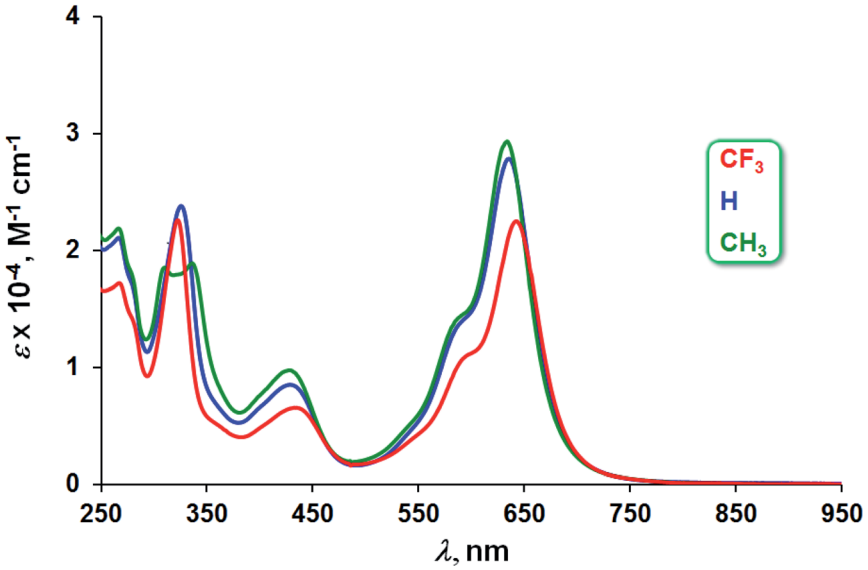

Fig. 3 UV-vis spectra of Au[XDPP] (X = CF_3, H, and CH_3) in dichloromethane.

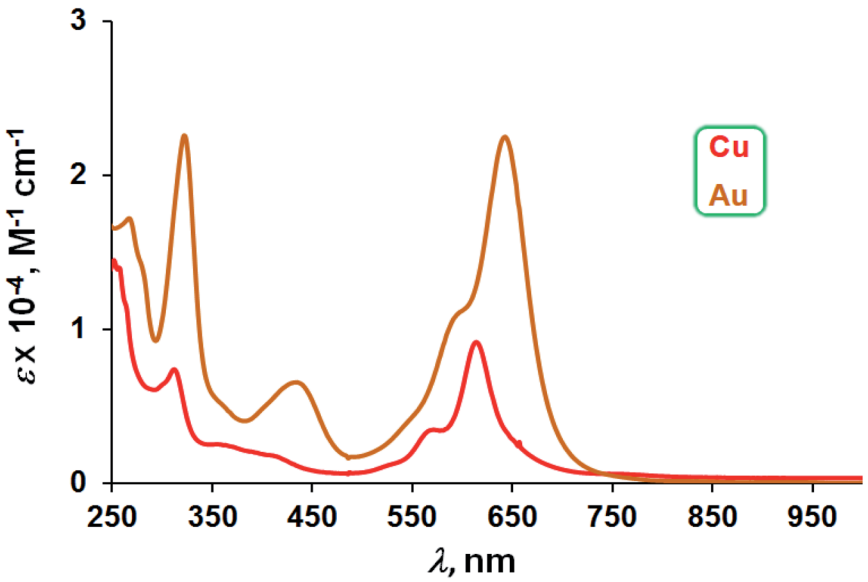

Fig. 4 UV-vis spectra of M[CF_3DPP] (M = Cu and Au) in dichloromethane.

3. Conclusion

The first Au(III) dipyrrin-bisphenolate complexes, Au[XDPP] with X = CF_3, H, and Me, have been synthesized in fair to good yields (50–77%) yields *via* the interaction of the corresponding free ligands and a threefold molar excess of Au(III) acetate in pyridine. X-ray structure analysis, optical spectroscopy, electrochemistry and DFT calculations all suggest an innocent Au^{III}–DPP^{3-} description for the complexes. The calculations, however, also suggest that while the compounds undergo ligand-centered oxidation, reduction occurs across both the Au($5d_{x^2-y^2}$) orbital and the DPP π-LUMO. In the latter respect, the Au–DPP complexes differ from simple Au corroles, which undergo exclusively corrole-centered reductions.

4. Experimental section

4.1. Materials and instruments

All reagents and solvents were used as purchased unless noted otherwise. Benzonitrile was distilled from P_4O_{10} and stored over activated 4 Å molecular sieves. Ultraviolet-visible (UV-vis) spectra were recorded in CH_2Cl_2 on an HP 8454 or a Varian Cary 50 spectrophotometer. Unless otherwise mentioned, ^1H (400 MHz) and ^{19}F (376 MHz) NMR spectra were recorded in

Open Access Article. Published on 02 January 2020. Downloaded on 2/22/2026 5:21:19 AM.
This article is licensed under a Creative Commons Attribution-NonCommercial 3.0 Unported Licence.

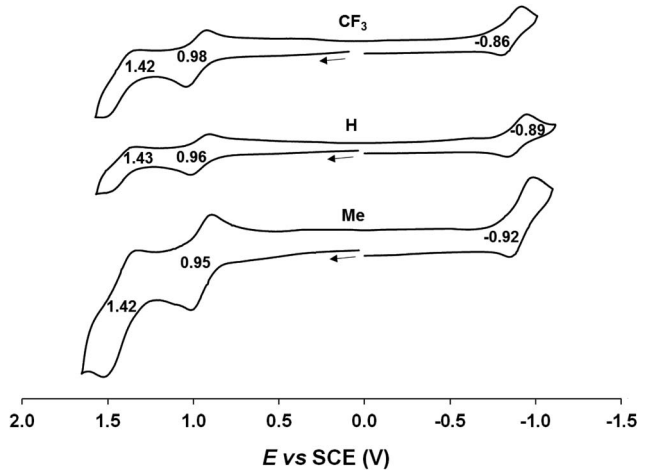

Fig. 5 Cyclic voltammograms of Au[XDPP] (X = CF_3, H and CH_3) in benzonitrile. Scan rate: 0.1 V s^{-1}.

$CDCl_3$ on a 400 MHz Bruker Avance III HD spectrometer equipped with a 5 mm BB/^{1}H (BB = ^{19}F, ^{31}P, and ^{15}N) SmartProbe and referenced to residual $CHCl_3$ (δ = 7.26 ppm) and 2,2,2-trifluoroethanol-d_3 (δ = −77.8 ppm), respectively. In the case of the free ligands, ^{1}H NMR spectra were recorded on a Bruker Avance III 500 spectrometer operating at 500 MHz and ^{19}F NMR spectra were recorded on a Bruker Avance III 600 spectrometer operating at 564 MHz and available at the PACSMUB-WPCM technological platform, which relies on the "Institut de Chimie Moléculaire de l'Université de Bourgogne" and Satt Sayens "TM", a Burgundy University private subsidiary. All NMR shift values are expressed as ppm. ^{1}H and ^{19}F spectra were calibrated using the residual peak of chloroform at 7.26 ppm or acetone-d_6 at 2.05 ppm. High-resolution electrospray ionization mass spectra were recorded on an LTQ Orbitrap XL spectrometer. MALDI-TOF mass spectra were recorded on a Bruker Ultraflex Extreme MALDI Tandem TOF Mass Spectrometer using dithranol as the matrix. Cyclic voltammetry was performed with an EG&G Model 263A potentiostat having a three-electrode system, including a glassy carbon working electrode, a platinum wire counter electrode, and a saturated calomel reference electrode (SCE). Tetra(*n*-butyl)ammonium perchlorate (TBAP) was recrystallized three times from absolute ethanol and dried *in vacuo* for at least one week prior to use as supporting electrolyte. The SCE was separated from the bulk solution by a fritted-glass bridge filled with the solvent/supporting-electrolyte mixture. Sample solutions in dry benzonitrile were purged with argon for at least 5 min prior to electrochemical measurements, which were also carried out under an argon blanket. All potentials are referenced to the SCE. The dipyrrin-bisanisole H_3[HDPPOMe] and the corresponding dipyrrin-bisphenol H_3[HDPP] were synthesized as described in the literature.[32]

4.2. General synthetic procedure for dipyrrin-bisanisoles

To a stirred solution of the appropriate benzaldehyde (0.86 mmol, 1.0 eq.) and 2-(2-methoxyphenyl)pyrrole (synthesized according to a literature procedure,[33] 299 mg, 1.73 mmol, 2.0 eq.) in CH_2Cl_2 (15 mL) under argon, trifluoroacetic acid (22 μL) was added and the mixture was stirred for 2 h at room temperature. 2,3-Dichloro-5,6-dicyano-1,4-benzoquinone (DDQ, 200 mg, 0.88 mmol) was then added and the resulting solution stirred overnight at room temperature. The reaction mixture was washed with saturated $NaHCO_3$ aqueous solution and extracted with CH_2Cl_2. The organic phase was dried over $MgSO_4$, evaporated to dryness, and subjected to column chromatography as described below.

4.3. H_3[CF_3DPPOMe]

This compound was purified by silica gel column using CH_2Cl_2 and a 9 : 1 mixture of CH_2Cl_2/MeOH as eluent and by alumina using a 2 : 3 mixture of CH_2Cl_2/heptane. Yield 281 mg

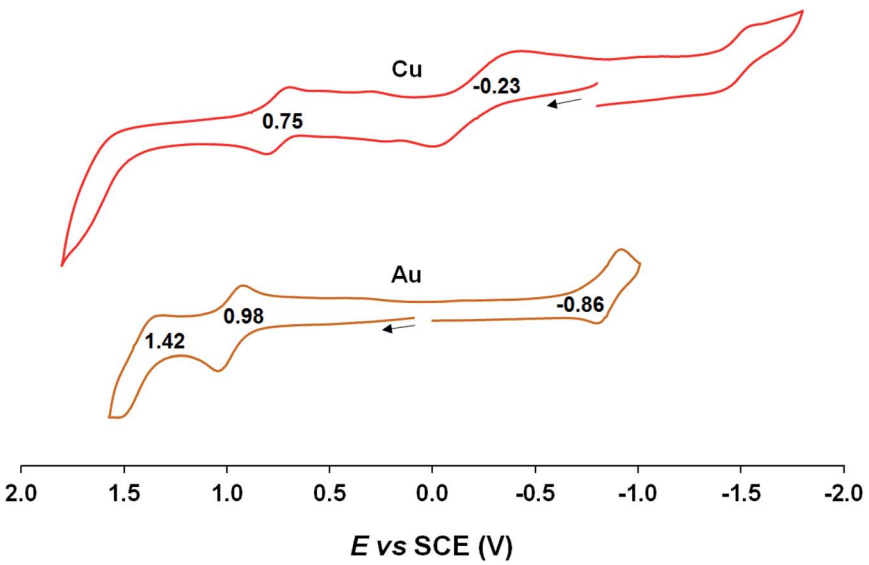

Fig. 6 Cyclic voltammograms of M[CF_3DPP] (M = Cu and Au) in benzonitrile. Scan rate: for Cu is 0.05 V s^{-1} and 0.1 V s^{-1} for Au.

 This journal is © The Royal Society of Chemistry 2020

Open Access Article. Published on 02 January 2020. Downloaded on 2/22/2026 5:21:19 AM.
This article is licensed under a Creative Commons Attribution-NonCommercial 3.0 Unported Licence.

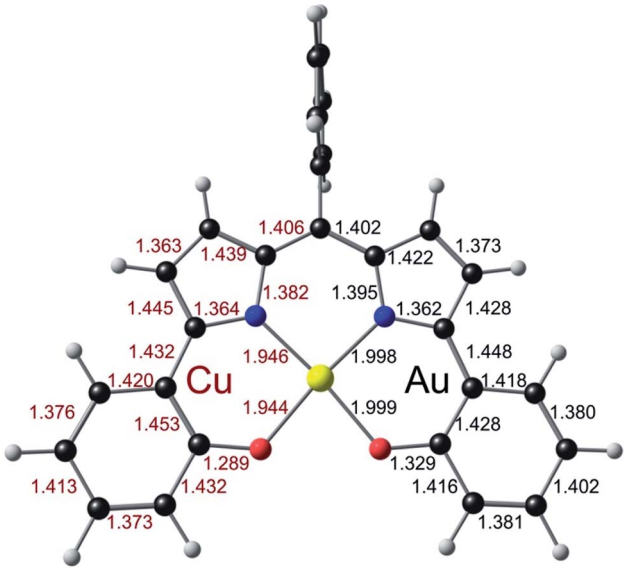

Fig. 7 Juxtaposition of the OLYP/STO-TZ2P optimized geometries (Å) Cu (left) and Au (right) DPP complexes.

(0.56 mmol, 65%). UV-vis λ_{max} [nm, $\varepsilon \times 10^4$ (M^{-1} cm^{-1})]: 526 (2.62), 610 (0.27). ^{1}H NMR δ ($CDCl_3$, $\delta = 7.26$ ppm): 13.66 (s, 1H, NH); 8.04 (d, 2H, $J = 7.5$ Hz, phenylmethoxy); 7.72 (d, 2H, $J =$ 8.0 Hz, *m* or *o* 10-*p*$CF_3C_6H_4$); 7.67 (d, 2H, $J = 8.0$ Hz, *m* or *o* 10-*p*$CF_3C_6H_4$); 7.35 (t, 2H, $J = 7.5$ Hz, phenylmethoxy); 7.05 (t, 2H, J = 7.5 Hz, phenylmethoxy); 7.00 (d, 2H, $J = 7.5$ Hz, phenylmethoxy); 6.94 (d, 2H, $J = 4.5$ Hz, β-H); 6.54 (d, 2H, $J = 4.5$ Hz, β-H); 3.87 (s, 6H, OMe). ^{19}F NMR δ: −62.96 (s, 3F, 10-*p*$CF_3C_6H_4$). LRMS (MALDI/TOF) $[M]^{+\bullet}$: 500.65 (expt), 500.17 (calcd). HRMS (ESI) $[M + H]^+$: 501.1781 (expt), 501.1784 (calcd).

4.4. H_3[MeDPPOMe]

This compound was purified by silica gel column using a 4 : 1 mixture of heptane/AcOEt as eluent. Yield 212 mg (0.47 mmol, 55%). UV-vis λ_{max} [nm, $\varepsilon \times 10^4$ (M^{-1} cm^{-1})]: 316 (2.08), 521 (2.96), 601 (0.60). ^{1}H NMR δ ($CDCl_3$, $\delta = 7.26$ ppm): 13.75 (s, 1H, NH); 8.06 (d, 2H, $J = 7.5$ Hz, phenylmethoxy); 7.45 (d, 2H, $J =$ 8.0 Hz, *m* or *o* 10-*p*MeC_6H_4); 7.35 (t, 2H, $J = 7.5$ Hz, phenylmethoxy); 7.27 (d, 2H, $J = 8.0$ Hz, *m* or *o* 10-*p*MeC_6H_4); 7.05 (t, 2H, $J = 7.5$ Hz, phenylmethoxy); 7.01 (d, 2H, $J = 7.5$ Hz, phenylmethoxy); 6.95 (d, 2H, $J = 4.5$ Hz, β-H); 6.67 (d, 2H, $J = 4.5$ Hz, β-H); 3.87 (s, 6H, OMe); 2.47 (s, 3H, CH_3). LRMS (MALDI/TOF) $[M]^{+\bullet}$: 446.58 (expt), 446.20 (calcd). HRMS (ESI) $[M + H]^+$: 447.2059 (expt), 447.2067 (calcd).

4.5. General synthetic procedure for dipyrrin-bisphenols

The experimental procedure was adapted from methodology described in the literature for the preparation of the unsubstituted phenyl ligand H_3[HDPP].[32] To a stirred solution of the corresponding dipyrrin-bisanisole (0.282 mmol) in CH_2Cl_2 (14 mL) under an argon atmosphere, BBr_3 (1.0 M in heptane, 5.63 mL, 5.63 mmol) was added at 0 °C. The reaction mixture was stirred and allowed to warm up to room temperature and left for 3 days before quenching with methanol (14 mL). Concentrated HCl (37%, 1.35 mL) was then added and the resulting mixture was refluxed for 3 h. After cooling, the mixture was neutralized with saturated aqueous $NaHCO_3$ and extracted with ethyl acetate. The organic layer was dried over $MgSO_4$ and evaporated to dryness; the residue was then subjected to column chromatography to yield the desired free dipyrrin-bisphenol ligands.

4.6. H_3[CF_3DPP]

The compound was purified by silica gel column using 3 : 1 heptane/ethyl acetate as eluent. Yield 58.6 mg (0.12 mmol, 44%). UV-vis λ_{max} [nm, $\varepsilon \times 10^4$ (M^{-1} cm^{-1})]: 301 (1.17), 545 (1.53), 612 (0.47). ^{1}H NMR δ (acetone-d_6, $\delta = 2.05$ ppm): 7.90 (d, 2H, $J = 8.0$ Hz, *m* or *o* 10-*p*$CF_3C_6H_4$); 7.87 (d, 2H, $J = 7.5$ Hz, phenoxy); 7.80 (d, 2H, $J = 8.0$ Hz, *m* or *o* 10-*p*$CF_3C_6H_4$); 7.30 (t, 2H, $J = 7.5$ Hz, phenoxy); 7.16 (m, 2H, β-H); 7.06 (d, 2H, $J =$ 7.5 Hz, phenoxy); 6.98 (t, 2H, $J = 7.5$ Hz, phenoxy); 6.67 (m, 2H, β-H). ^{19}F NMR δ: −63.01 (s, 3F, 10-*p*$CF_3C_6H_4$). LRMS (MALDI/TOF) $[M]^{+\bullet}$: 472.64 (expt), 472.14 (calcd). HRMS (ESI) $[M + H]^+$: 473.1459 (expt), 473.1471 (calcd).

4.7. H_3[MeDPP]

The compound was purified by silica gel column using a 4 : 1 heptane/ethyl acetate as eluent. Yield 89.2 mg (0.213 mmol, 75%). UV-vis λ_{max} [nm, $\varepsilon \times 10^4$ (M^{-1} cm^{-1})]: 323 (1.27), 373 (0.53), 545 (2.04), 601 (0.52). ^{1}H NMR δ (acetone-d_6, $\delta = 2.05$ ppm): 7.86 (d, 2H, $J = 7.5$ Hz, phenoxy); 7.46 (d, 2H, $J = 8.0$ Hz, *m* or *o* 10-*p*MeC_6H_4); 7.37 (t, 2H, $J = 8.0$ Hz, *m* or *o* 10-*p*MeC_6H_4); 7.27 (t, 2H, $J = 7.5$ Hz, phenoxy); 7.13 (d, 2H, $J = 4.5$ Hz, β-H); 7.03 (d, 2H, $J = 7.5$ Hz, phenoxy); 6.95 (t, 2H, $J = 7.5$ Hz, phenoxy); 6.75 (m, 2H, β-H); 2.48 (s, 3H, CH_3). LRMS (MALDI/TOF)

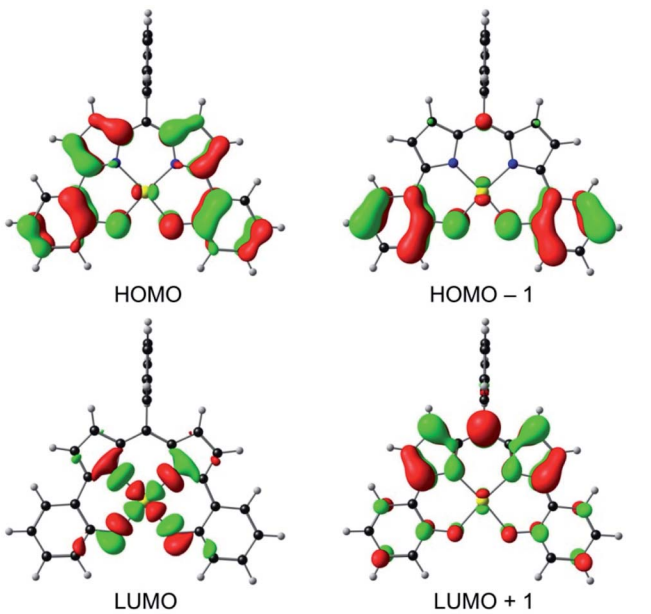

Fig. 8 OLYP/STO-TZ2P frontier MOs of Au[DPP] under a C_{2v} symmetry constraint.

Open Access Article. Published on 02 January 2020. Downloaded on 2/22/2026 5:21:19 AM.
This article is licensed under a Creative Commons Attribution-NonCommercial 3.0 Unported Licence.

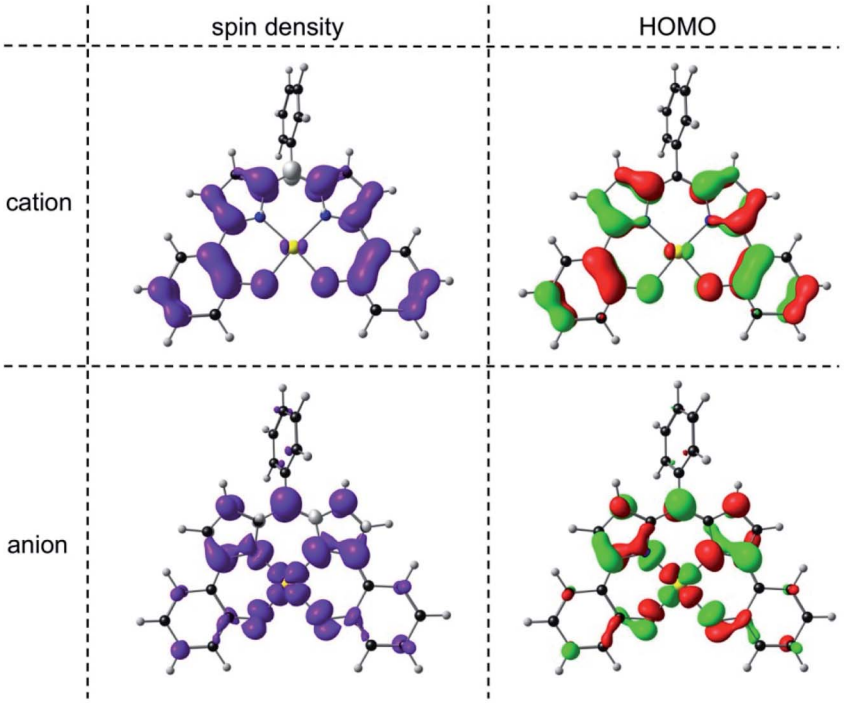

Fig. 9 OLYP/STO-TZ2P spin density and HOMO profiles of the cationic and anionic states of Au[DPP] optimized with a C_2 symmetry constraint.

$[M]^{+\bullet}$: 418.55 (expt), 418.17 (calcd). HRMS (ESI) $[M + H]^+$: 419.1748 (expt), 419.1754 (calcd).

4.8. General synthetic procedure for gold dipyrrin-bisphenolates

Gold acetate (3 equiv.) was added to a pink solution of the free dipyrrin-bisphenol ligand (30 mg) in pyridine (6 mL). The resulting suspension was stirred for 24 h and monitored with TLC and mass spectrometry. The blue suspension that was finally obtained was passed through Celite, the resulting solution was filtered, and the filtrate was rotary-evaporated to dryness. The brown residue obtained was dissolved in THF or $CHCl_3$ and filtered twice through a double-layer of filter paper. The resulting blue filtrate was rotary-evaporated to yield a blue solid, which was thoroughly washed with *n*-hexane and dried under vacuum. Unfortunately, the compounds proved quite light-sensitive, especially in the presence of air, preventing us from obtaining satisfactory elemental analyses. Fortunately, X-ray quality crystals could be obtained for Au[CF_3DPP] *via* slow diffusion of methanol into a concentrated chloroform solution in about 2 weeks.

4.9. Au[CF_3DPP]

Yield 21 mg (0.031 mmol, 50%). UV-vis λ_{max} [nm, $\varepsilon \times 10^4$ (M^{-1} cm^{-1})]: 322 (2.26), 435 (0.65), 643 (2.25). ^{1}H NMR δ (1,1,2,2-tetrachloroethane-d_2, δ = 6.00 ppm): 7.82 (d, 2H, J = 8.0 Hz, *m* or *o*-10-*p*$CF_3C_6H_4$); 7.78 (d, 2H, J = 7.8 Hz, phenoxy); 7.71 (d, 2H, J = 8.0 Hz, *o* or *m*-10-*p*CF_3Ph); 7.39 (t, 2H, J = 7.8 Hz, phenoxy); 7.32 (d, 2H, J = 8.2 Hz, phenoxy); 7.25 (d, 2H, J = 4.8 Hz, β-H); 6.96 (t, 2H, J = 7.4 Hz, phenoxy); 6.83 (d, 2H, J = 4.8 Hz, β-H). ^{19}F NMR δ: −63.16 (s, 2F, 10-*p*$CF_3C_6H_4$); −63.18 (s, 1F, 10-*p*$CF_3C_6H_4$). HRMS (ESI, major isotopomer) $[M]^+$: 666.0789 (expt), 666.0824 (calcd).

4.10. Au[HDPP]

Yield 23 mg (0.038 mmol, 52%). UV-vis λ_{max} [nm, $\varepsilon \times 10^4$ (M^{-1} cm^{-1})]: 325 (2.38), 429 (0.85), 636 (2.79). ^{1}H NMR δ: 7.71 (d, 2H, J = 8.0 Hz, phenoxy); 7.56 to 7.50 (d, 5H, Ph), 7.33 to 7.28 (m, 4H, phenoxy); 7.16 (d, 2H, J = 4.8 Hz, β-H), 6.91 to 6.85 (m, 2H, phenoxy), 6.83 (d, 2H, J = 4.8 Hz, β-H). HRMS (ESI, major isotopomer) $[M]^+$: 598.0926 (expt), 598.0950 (calcd).

4.11. Au[MeDPP]

Yield 34 mg (0.055 mmol, 77%). UV-vis λ_{max} [nm, $\varepsilon \times 10^4$ (M^{-1} cm^{-1})]: 310 (1.85), 336 (1.89), 427 (0.97), 634 (2.93). ^{1}H NMR δ (1,1,2,2-tetrachloroethane-d_2, δ = 6.00 ppm): δ 7.77 (d, 2H, J = 7.8 Hz, phenoxy); 7.44 (d, 2H, J = 7.9 Hz, *m* or *o*-10-*p*$CH_3C_6H_4$), 7.39 to 7.30 (m, 4H, phenoxy; 2H, *o* or *m*-10-*p*$CH_3C_6H_4$); 7.24 (d, 2H, J = 4.7 Hz, β-H), 6.97 to 6.92 (overlapping d, 2H, J = 4.7 Hz, β-H and t, 2H, J = 7.8 Hz, phenoxy), 2.49 (3H, CH_3, 10-*p*$CH_3C_6H_4$). HRMS (ESI, major isotopomer) $[M]^+$: 612.1096 (expt), 612.1107 (calcd).

4.12. Synthesis of Cu[CF_3DPP]

Copper acetate (11 mg, 0.055 mmol, 5 equiv.) was added to a pink solution of the H_3[CF_3DPP] ligand (5 mg, 0.011 mmol) in pyridine (2 mL). The suspension was stirred for 1 h, at the end of which the reaction was complete, as indicated by TLC ($CHCl_3$-

 This journal is © The Royal Society of Chemistry 2020

Open Access Article. Published on 02 January 2020. Downloaded on 2/22/2026 5:21:19 AM.
This article is licensed under a Creative Commons Attribution-NonCommercial 3.0 Unported Licence.

2% CH_3OH) and mass spectrometry. The blue suspension obtained was filtered through Celite and the resulting solution was filtered twice before evaporation under vacuum. Yield 5.5 mg (0.010 mmol, 91%). UV-vis λ_{max} [nm, $\varepsilon \times 10^4$ (M^{-1} cm^{-1})]: 312 (0.74), 572 (0.35), 614 (0.92). HRMS (ESI, major isotopomer) $[M + H]^+ = 533.0527$ (expt), 533.0533 (calcd).

4.13. X-ray structure determination

X-ray diffraction data were collected on beamline 12.2.1 at the Advanced Light Source of Lawrence Berkeley National Laboratory, Berkeley, California. The samples were mounted on MiTeGen® kapton loops and placed in a 100(2) K nitrogen cold stream provided by an Oxford Cryostream 700 Plus low temperature apparatus on the goniometer head of a Bruker D8 diffractometer equipped with PHOTONII CPAD detector. Diffraction data were collected using synchrotron radiation monochromated with silicon(111) to a wavelength of 0.7288(1) Å. In each case, an approximate full-sphere of data was collected using 1° ω scans. Absorption corrections were applied using SADABS.[34] The structure was solved by intrinsic phasing (SHELXT)[35] and refined by full-matrix least squares on F^2 (SHELXL-2014)[36] using the ShelXle GUI.[37] Appropriate scattering factors were applied using the XDISP[38] program within the WinGX suite.[39] All non-hydrogen atoms were refined anisotropically. Hydrogen atoms were geometrically calculated and refined as riding atoms.

4.14. Computational methods

DFT calculations were carried out at the scalar-relativistic level with the ZORA (Zeroth Order Regular Approximation to the Dirac equation)[40–42] Hamiltonian, the OLYP[28,29] exchange-correlation functional, and all-electron ZORA STO-TZ2P relativistic basis sets, all as implemented in the ADF program system.[43,44]

Conflicts of interest

There are no conflicts of interest to declare.

Acknowledgements

This work was supported by the Research Council of Norway (grant no. 263332 to AG), the CNRS (UMR UB-CNRS 6302), the "Université Bourgogne Franche-Comté", the FEDER-FSE Bourgogne 2014/2020 (European Regional Development Fund), the "Conseil Régional de Bourgogne" (through the PARI II CDEA project), the National Research Fund of the Republic of South Africa (grant numbers 113327 and 96111 to JC), and the Advanced Light Source, Berkeley, California. The Advanced Light Source is supported by the Director, Office of Science, Office of Basic Energy Sciences, of the U.S. Department of Energy under Contract No. DE-AC02-05CH11231. The authors warmly thank Mrs Sandrine Pacquelet for technical assistance.

References

1 W. Shan, N. Desbois, S. Pacquelet, S. Brandès, Y. Rousselin, J. Conradie, A. Ghosh, C. P. Gros and K. M. Kadish, *Inorg. Chem.*, 2019, **58**, 7677–7689.
2 (*a*) K. E. Thomas, A. B. Alemayehu, J. Conradie, C. M. Beavers and A. Ghosh, *Acc. Chem. Res.*, 2012, **45**, 1203–1214; (*b*) A. Ghosh, *Chem. Rev.*, 2017, **117**, 3798–3881; (*c*) S. Ganguly and A. Ghosh, *Acc. Chem. Res.*, 2019, **52**, 2003–2014.
3 S. Nardis, F. Mandoj, M. Stefanelli and R. Paolesse, *Coord. Chem. Rev.*, 2019, **388**, 360–405.
4 (*a*) S. Ganguly, D. Renz, L. J. Giles, K. J. Gagnon, L. J. McCormick, J. Conradie, R. Sarangi and A. Ghosh, *Inorg. Chem.*, 2017, **56**, 14788–14800; (*b*) S. Ganguly, J. Conradie, J. Bendix, K. J. Gagnon, L. J. McCormick and A. Ghosh, *J. Phys. Chem. A*, 2017, **121**, 9589–9598.
5 X. Jiang, W. Shan, N. Desbois, V. Quesneau, S. Brandès, E. Van Caemelbecke, W. R. Osterloh, V. Blondeau-Patissier, C. P. Gros and K. M. Kadish, *New J. Chem.*, 2018, **42**, 8220–8229.
6 For selected references to ligand noninnocence in Cu corroles, see: (*a*) I. H. Wasbotten, T. Wondimagegn and A. Ghosh, *J. Am. Chem. Soc.*, 2002, **124**, 8104–8116; (*b*) C. Brückner, R. P. Briñas and J. A. K. Bauer, *Inorg. Chem.*, 2003, **42**, 4495–4497; (*c*) M. Bröring, F. Bregier, E. C. Tejero, C. Hell and M. C. Holthausen, *Angew. Chem., Int. Ed.*, 2007, **46**, 445–448; (*d*) K. E. Thomas, I. H. Wasbotten and A. Ghosh, *Inorg. Chem.*, 2008, **47**, 10469–10478; (*e*) A. B. Alemayehu, E. Gonzalez, L.-K. Hansen and A. Ghosh, *Inorg. Chem.*, 2009, **48**, 7794–7799; (*f*) A. B. Alemayehu, L.-K. Hansen and A. Ghosh, *Inorg. Chem.*, 2010, **49**, 7608–7610; (*g*) K. E. Thomas, J. Conradie, L.-K. Hansen and A. Ghosh, *Eur. J. Inorg. Chem.*, 2011, 1865–1870; (*h*) S. Berg, K. E. Thomas, C. M. Beavers and A. Ghosh, *Inorg. Chem.*, 2012, **51**, 9911–9916; (*i*) K. E. Thomas, L. J. McCormick, D. Carrié, H. Vazquez-Lima, G. Simmoneaux and A. Ghosh, *Inorg. Chem.*, 2018, **57**, 4270–4276; (*j*) I. K. Thomassen, L. J. McCormick and A. Ghosh, *ACS Omega*, 2018, **3**, 5106–5110; (*k*) H. Lim, K. E. Thomas, B. Hedman, K. O. Hodgson, A. Ghosh and E. I. Solomon, *Inorg. Chem.*, 2019, **58**, 6722–6730.
7 A. Kochem, L. Chiang, B. Baptiste, C. Philouze, N. Leconte, O. Jarjayes, T. Storr and F. Thomas, *Chem.–Eur. J.*, 2012, **18**, 14590–14593.
8 Y. Feng, L. A. Burns, L.-C. Lee, C. D Sherrill and C. W. Jones, *Inorg. Chim. Acta*, 2015, **430**, 30–35.
9 L. Lecarme, A. Kochem, L. Chiang, J. Moutet, F. Berthiol, C. Philouze, N. Leconte, T. Storr and F. Thomas, *Inorg. Chem.*, 2018, **57**, 9708–9719.
10 Z. Gross and H. B. Gray, *Adv. Synth. Catal.*, 2004, **346**, 165–170.
11 N. Levy, A. Mahammed, M. Kosa, D. T. Major, Z. Gross and L. Elbaz, *Angew. Chem., Int. Ed.*, 2015, **54**, 14080–14084.
12 K. E. Thomas, A. B. Alemayehu, J. Conradie, C. M. Beavers and A. Ghosh, *Inorg. Chem.*, 2011, **50**, 12844–12851.

Open Access Article. Published on 02 January 2020. Downloaded on 2/22/2026 5:21:19 AM.
This article is licensed under a Creative Commons Attribution-NonCommercial 3.0 Unported Licence.

13 First reports of Au corroles: (*a*) A. B. Alemayehu and A. Ghosh, *J. Porphyrins Phthalocyanines*, 2011, **15**, 106–110; (*b*) E. Rabinovich, I. Goldberg and Z. Gross, *Chem.–Eur. J.*, 2011, **17**, 12294–12301.

14 (*a*) K. E. Thomas, C. M. Beavers and A. Ghosh, *Mol. Phys.*, 2012, **110**, 2439–2444; (*b*) J. Capar, J. Zonneveld, S. Berg, J. Isaksson, K. J. Gagnon, K. E. Thomas and A. Ghosh, *J. Inorg. Biochem.*, 2016, **162**, 146–153; (*c*) W. Sinha, M. G. Sommer, M. van der Meer, S. Plebst, B. Sarkar and S. Kar, *Dalton Trans.*, 2016, **45**, 2914–2923; (*d*) K. Sudhakar, A. Mizrahi, M. Kosa, N. Fridman, B. Tumanskii, M. Saphier and Z. Gross, *Angew. Chem., Int. Ed.*, 2017, **56**, 9837–9841; (*e*) K. E. Thomas, K. J. Gagnon, L. J. McCormick and A. Ghosh, *J. Porphyrins Phthalocyanines*, 2018, **22**, 596–601.

15 Note that silver corroles may be innocent or noninnocent, depending on the substitution pattern: (*a*) R. Sarangi, L. J. Giles, K. E. Thomas and A. Ghosh, *Eur. J. Inorg. Chem.*, 2016, 3225–3227; (*b*) K. E. Thomas, H. Vazquez-Lima, Y. Fang, Y. Song, K. J. Gagnon, C. M. Beavers, K. M. Kadish and A. Ghosh, *Chem.–Eur. J.*, 2015, **21**, 16839–16847.

16 L. Lecarme, A. Kochem, L. Chiang, J. Moutet, F. Berthiol, C. Philouze, N. Leconte, T. Storr and F. Thomas, *Inorg. Chem.*, 2018, **57**, 9708–9719.

17 M. Yamamura, H. Takizawa, Y. Gobo and T. Nabeshima, *Dalton Trans.*, 2016, **45**, 6834–6838.

18 M. Yamamura, M. Albrecht, M. Albrecht, Y. Nishimura, T. Arai and T. Nabeshima, *Inorg. Chem.*, 2014, **53**, 1355–1360.

19 S. Rausaria, A. Kamadulski, N. P. Rath, L. Bryant, Z. Chen, D. Salvemini and W. L. Neumann, *J. Am. Chem. Soc.*, 2011, **133**, 4200–4203.

20 S. El Ghachtouli, K. Wójcik, L. Copey, F. Szydlo, E. Framery, C. Goux-Henry, L. Billon, M.-F. Charlot, R. Guillot, B. Andrioletti and A. Aukauloo, *Dalton Trans.*, 2011, **40**, 9090–9093.

21 M. Saikawa, M. Daicho, T. Nakamura, J. Uchida, M. Yamamura and T. Nabeshima, *Chem. Commun.*, 2016, **52**, 4014–4017.

22 T. Ohkawara, K. Suzuki, K. Nakano, S. Mori and K. Nozaki, *J. Am. Chem. Soc.*, 2014, **136**, 10728–10735.

23 M. Yamamura, H. Takizawa, N. Sakamoto and T. Nabeshima, *Tetrahedron Lett.*, 2013, **54**, 7049–7052.

24 A. Sumiyoshi, Y. Chiba, R. Matsuoka, T. Noda and T. Nabeshima, *Dalton Trans.*, 2019, **48**, 13169–13175.

25 Unlike Au corroles,[26] the compounds do not exhibit NIR phosphorescence in common organic solvents, including toluene and dichloromethane.

26 A. B. Alemayehu, N. U. Day, T. Mani, A. B. Rudine, K. E. Thomas, O. A. Gederaas, S. A. Vinogradov, C. C. Wamser and A. Ghosh, *ACS Appl. Mater. Interfaces*, 2016, **8**, 18935–18942.

27 The relative constancy of the oxidation potential with respect to the substituent X suggests that the HOMO does not have much of an amplitude at the *meso* position. This is indeed the case, as shown later in the paper.

28 The OPTX exchange functional: N. C. Handy and A. J. Cohen, Left-right correlation energy, *Mol. Phys.*, 2001, **99**, 403–412.

29 The LYP correlation functional: C. T. Lee, W. T. Yang and R. G. Parr, Development of the Colle-Salvetti correlation-energy formula into a functional of the electron-density, *Phys. Rev. B: Condens. Matter Mater. Phys.*, 1988, **37**, 785–789.

30 Early studies from one of our laboratories established that DFT calculations generally do an excellent job of describing the ionization potentials and cationic states of porphyrin-type molecules: (*a*) A. Ghosh and J. Almlöf, *Chem. Phys. Lett.*, 1993, **213**, 519–521; (*b*) A. Ghosh, *J. Am. Chem. Soc.*, 1995, **117**, 4691–4699; (*c*) A. Ghosh and T. Vangberg, *Theor. Chem. Acc.*, 1997, **97**, 143–149; (*d*) A. Ghosh, *Acc. Chem. Res.*, 1998, **31**(4), 189–198; (*e*) A. Ghosh, T. Wondimagegn and A. B. J. Parusel, *J. Am. Chem. Soc.*, 2000, **122**, 5100–5104; (*f*) A. Ghosh and E. Steene, *J. Biol. Inorg Chem.*, 2001, **6**, 739–752.

31 The electron affinities and anionic states of porphyrin-type molecules have been less explored by means of DFT calculations. Nevertheless, the available data suggest that DFT does a good job of tackling the question of metal *versus* ligand-centered reduction. See, *e.g.*: H. Ryeng, E. Gonzalez and A. Ghosh, *J. Phys. Chem. B*, 2008, **112**, 15158–15173.

32 C. Ikeda, S. Ueda and T. Nabeshima, *Chem. Commun.*, 2009, 2544–2546.

33 R. D. Rieth, N. P. Mankad, E. Calimano and J. P. Sadighi, *Org. Lett.*, 2004, **6**, 3981–3983.

34 L. Krause, R. Herbst-Irmer, G. M. Sheldrick and D. Stalke, *J. Appl. Crystallogr.*, 2015, **48**, 3–10.

35 G. M. Sheldrick, *Acta Crystallogr., Sect. A: Found. Adv.*, 2015, **71**, 3–8.

36 G. M. Sheldrick, *Acta Crystallogr., Sect. C: Struct. Chem.*, 2015, **71**, 3–8.

37 C. B. Hübschle, G. M. Sheldrick and B. Dittrich, *J. Appl. Crystallogr.*, 2011, **44**, 1281–1284.

38 L. Kissel and R. H. Pratt, *Acta Crystallogr., Sect. A: Found. Crystallogr.*, 1990, **46**, 170–175.

39 L. J. Farrugia, *J. Appl. Crystallogr.*, 2012, **45**, 849–854.

40 E. van Lenthe, E. J. Baerends and J. G. Snijders, *J. Chem. Phys.*, 1993, **99**, 4597–4610.

41 E. van Lenthe, E. J. Baerends and J. G. Snijders, *J. Chem. Phys.*, 1994, **101**, 9783–9792.

42 E. van Lenthe, A. Ehlers and E. J. Baerends, *J. Chem. Phys.*, 1999, **110**, 8943–8953.

43 G. te Velde, F. M. Bickelhaupt, S. J. A. van Gisbergen, C. F. Guerra, E. J. Baerends, J. G. Snijders and T. Ziegler, *J. Comput. Chem.*, 2001, **22**, 931–967.

44 C. F. Guerra, J. G. Snijders, G. te Velde and E. J. Baerends, *Theor. Chem. Acc.*, 1998, **99**, 391–403.

 This journal is © The Royal Society of Chemistry 2020